

Role of Chains in the Formation of Extended Framework Tin(II) Phosphates and Related Materials

Brian A. Adair, S. Neeraj, and Anthony K. Cheetham*

Materials Research Laboratory, University of California, Santa Barbara, California 93106

Received June 10, 2002. Revised Manuscript Received January 27, 2003

The reactions of tin(II) chloride with phosphonic and phosphinic acids under hydrothermal conditions result in structures with varying dimensionalities. The synthesis and characterization of eight new structures is described. $\text{SnCl}(\text{HPhPO}_2)$, **I**, triclinic, $P\bar{1}$ (No. 2), has lattice parameters $a = 5.4767(6)$ Å, $b = 8.8106(9)$ Å, $c = 9.5219(10)$ Å, $\alpha = 104.564(2)^\circ$, $\beta = 95.440(2)^\circ$, $\gamma = 99.349(2)^\circ$, and $V = 434.34(8)$ Å³. $(\text{SnCl})_2\text{MePO}_3$, **II**, triclinic, $P\bar{1}$ (No. 2), has $a = 4.7275(17)$ Å, $b = 6.152(2)$ Å, $c = 13.632(5)$ Å, $\alpha = 81.299(7)^\circ$, $\beta = 89.052(7)^\circ$, $\gamma = 89.781(7)^\circ$, and $V = 391.8(3)$ Å³. $\text{Sn}_2\text{Cl}(\text{EtPO}_3)\text{EtPO}_2\text{OH}$, **III**, monoclinic, $P2_1/m$ (No. 11), has $a = 4.814(4)$ Å, $b = 8.530(4)$ Å, $c = 15.214(8)$ Å, $\beta = 99.09(10)^\circ$, and $V = 616.9(7)$ Å³. $\beta\text{-SnEtPO}_3$, **IV**, monoclinic, Cc (No. 9), has $a = 4.6415(13)$ Å, $b = 18.695(5)$ Å, $c = 6.4964(18)$ Å, $\beta = 99.907(4)^\circ$, and $V = 555.3(3)$ Å³. SnMePO_3 , **V**, monoclinic, $P2_1/c$ (No. 14), has $a = 4.5998(7)$ Å, $b = 15.430(2)$ Å, $c = 6.5861(10)$ Å, $\beta = 100.719(3)^\circ$, and $V = 459.30(12)$ Å³. $\text{Sn}_2(\text{O}_3\text{P}(\text{CH}_2)_2\text{PO}_3)$, **VI**, monoclinic, $P2_1/c$ (no. 14), has $a = 4.6435(6)$ Å, $b = 13.4512(16)$ Å, $c = 6.4767(8)$ Å, $\beta = 100.258(2)^\circ$, and $V = 398.07(9)$ Å³. $\text{SnPO}_3\text{CH}_2\text{COOH}$, **VII**, monoclinic, $P2_1/n$ (No. 14), has $a = 5.490(2)$ Å, $b = 4.890(2)$ Å, $c = 21.884(9)$ Å, $\beta = 90.505(7)^\circ$, and $V = 587.4(4)$ Å³. $(\text{NH}_4)_2\text{Sn}(\text{O}_3\text{PCH}_2\text{PO}_3)$, **VIII**, orthorhombic, $Pbca$ (No. 61), has $a = 10.3417(10)$ Å, $b = 10.0475(10)$ Å, $c = 16.9927(17)$ Å, and $V = 1765.7(3)$ Å³. For the first time, a three-ring (3R) phosphonate chain and an open-chain (i.e., no rings) phosphinate “wire” have been isolated. The phosphate analogues of these structures serve as key structural motifs in tin(II), zinc(II), and cobalt(II) phosphates, underscoring their role in the formation of framework phosphates. We propose that metal phosphate wires could play an important role in the formation of open-framework materials.

Introduction

The past two decades have witnessed a tremendous surge of interest in extended inorganic solids with open framework structures (OFs). In addition to the well-known OF aluminosilicate zeolites and aluminophosphates (AlPOs), many other classes of OFs have been discovered, for example, transition metal phosphates, metal sulfides, nitrides, and halides.¹ In certain circumstances, these OFs can be rendered nanoporous and exploited in catalysis, sorption, and separations.^{2–4} Despite advances in synthesizing frameworks with novel open architectures, the mechanistic details of the hydrothermal reaction processes commonly used in their synthesis remain unclear. Characterizing labile intermediates *ex situ* has proven difficult since the multistep and competing reactions have rapid kinetics; for example, the half-life of crystallization of gallophosphate (GaPO) ULM-5 is on the order of 1 min.⁵ Thus, if the reaction mixture is quenched, intermediates may trans-

form during the workup procedure owing to their reactive nature, and frequently only powders or amorphous gels are obtained.⁵ This can be circumvented by choosing a solvent that lowers the reactivity of the intermediates.⁶ In an alternative strategy, recent *in situ* XRD and NMR experiments with GaPOs and AlPOs have shed light on the nature of intermediate species in solution.^{5,7,8}

Proposed mechanisms for the formation of metal phosphates have focused primarily on gallium, aluminum, and zinc phosphates. The *in situ* NMR experiments of Taullelle et al. support the existence of Al_2P_2 four-rings (4Rs) in solution,⁸ and Férey has proposed that the formation of the ULM-*n* family of GaPOs and AlPOs occurs via condensation of molecular building units (MBUs).⁹ Roesky and co-workers and Mason and co-workers have made a number of inorganic/organic analogues of secondary building units (SBUs) found in zeolites and OF phosphates.¹⁰ Al_2P_2 one-dimensional (1D) chains, made up of cornered-shared 4Rs bearing

* To whom correspondence should be addressed.

(1) Cheetham, A. K.; Loiseau, T.; Férey, G. *Angew. Chem., Int. Ed.* **1999**, *38*, 3268.

(2) Thomas, J. M. *Angew. Chem., Int. Ed. Engl.* **1994**, *33*, 913.

(3) Herron, N.; Farneth, W. E. *Adv. Mater.* **1996**, *8*, 959.

(4) Arends, I. W. C. E.; Sheldon, R. A.; Wallau, M.; Schuchardt, U. *Angew. Chem., Int. Ed. Engl.* **1997**, *36*, 1144.

(5) Francis, R. J.; O'Brian, S.; Fogg, A. M.; Halasyamani, P. S.; O'Hare, D.; Loiseau, D. B.; Férey, G. *J. Am. Chem. Soc.* **1999**, *121*, 1002.

(6) (a) Oliver, S.; Kuperman, A.; Lough, A.; Ozin, G. A. *Inorg. Chem.* **1996**, *35*, 6373. (b) Oliver, S.; Kuperman, A.; Lough, A.; Ozin, G. A. *Chem. Mater.* **1996**, *8*, 2391. (c) Jones, R. H.; Thomas, J. M.; Xu, R.; Huo, Q.; Xu, Y.; Cheetham, A. K.; Bieber, D. *J. Chem. Soc., Chem. Commun.* **1990**, 1170.

(7) Walton, R. I.; Millange, F.; O'Hare, D.; Paulet, C.; Loiseau, D. B.; Férey, G. *Chem. Mater.* **2000**, *12*, 1977.

(8) Taullelle, F.; Haouas, M.; Gerardin, C.; Estournes, C.; Loiseau, D. B.; Férey, G. *Colloids Surf., A* **1999**, *158*, 229.

(9) Férey, G. *J. Fluorine Chem.* **1995**, *72*, 187.

Table 1^a

	gel composition	T (K)	t (h)	product composition
I	1:1:30 $\text{SnCl}_2 \cdot 2\text{H}_2\text{O} \cdot \text{PhHPO}_2\text{H} \cdot \text{H}_2\text{O}$	423	48	$\text{SnCl}(\text{HPhPO}_2)$
II	1:1:30 $\text{SnCl}_2 \cdot 2\text{H}_2\text{O} \cdot \text{MePO}_3\text{H}_2 \cdot \text{H}_2\text{O}$	423	48	$(\text{SnCl})_2\text{MePO}_3$
III	1:1:30 $\text{SnCl}_2 \cdot \text{EtPO}_3\text{H}_2 \cdot \text{H}_2\text{O}$	423	48	$\text{Sn}_2\text{Cl}(\text{EtPO}_3)\text{EtPO}_2\text{OH}$
IV	1:1:300 $\text{SnCl}_2 \cdot 2\text{H}_2\text{O} \cdot \text{MePO}_3\text{H}_2 \cdot \text{H}_2\text{O}$	423	48	$\beta\text{-SnEtPO}_3$
V	1:1:300 $\text{SnCl}_2 \cdot 2\text{H}_2\text{O} \cdot \text{EtPO}_3\text{H}_2 \cdot \text{H}_2\text{O}$	423	48	SnMePO_3
VI	1:1:450 $\text{SnC}_2\text{O}_4 \cdot \text{H}_2\text{O}_3 \cdot \text{PCH}_2\text{CH}_2\text{PO}_3\text{H}_2 \cdot \text{H}_2\text{O}$	433	24	$\text{Sn}_2(\text{O}_3\text{P}(\text{CH}_2)_2\text{PO}_3)$
VII	1:1:450 $\text{SnC}_2\text{O}_4 \cdot (\text{C}_2\text{O}_2\text{H}_3\text{PO}_3\text{H}_2 \cdot \text{H}_2\text{O})$	433	24	$\text{SnPO}_3\text{CH}_2\text{COOH}$
VIII	1:1:4:1.8:100:50 $\text{SnC}_2\text{O}_4 \cdot \text{H}_2\text{O}_3 \cdot \text{PCH}_2\text{PO}_3\text{H}_2 \cdot \text{GC} \cdot \text{H}_2\text{O} \cdot \text{EG}$	433	60	$(\text{NH}_4)_2\text{Sn}(\text{O}_3\text{PCH}_2\text{PO}_3)$

^a Ph = C₆H₅, Me = CH₃, Et = CH₃CH₂, GC = guanidine carbonate, EG = ethylene glycol.

terminal Al–OH and P–OH groups, have been isolated from tetraethylene glycol.^{6c} In contrast to the MBU model, Ozin and co-workers postulate that these infinite chains are the progenitors of two-dimensional (2D) layers and three-dimensional (3D) frameworks on hydrolysis and condensation.¹¹ Finally, Rao and co-workers postulate that the 1D corner-sharing chains arise from monomeric M₂P₂ 4Rs and report the isolation and transformation of zinc phosphate rings to 1D, 2D, and 3D structures.¹²

A number of OF tin(II) phosphates (SnPOs) have recently been reported.¹³ These systems tend to be topologically less complex with regard to the metal connectivity than other metal phosphates since the tin centers are usually only three-connected (via oxygen). Thus, to study metal phosphate reaction pathways, we looked at the simpler SnPO system. If a phosphonic acid (RPO₃H₂) instead of phosphoric acid is reacted with [Sn²⁺], the three oxygens of the RPO₃ units limit the connectivity of the phosphorus atom to the metal centers, thereby increasing the chance of forming even less complex materials. The hope, then, is two-fold: first, that the reaction pathway of even simpler tin(II) phosphonates (SnRPOs) can be deduced; and second, that this pathway may be applicable to SnPO and other metal phosphates systems. This theme of limiting the connectivity can be extended further. Controlling the hydrolysis of the tin(II) reagent can yield [SnO₂X] units (e.g., X = F, Cl); using substituted phosphinic acid instead of phosphonic acid gives rise to RR'PO₂ units. Both units are, at most, two-connected. In the present work, a systematic investigation of the tin(II) chloride phosphonate and phosphinate systems reveals the clear evolution of closely related architectures, from 1D wires (i.e., SnCl(HPhPO₂), **I**) to 1D chains (i.e., (SnCl)₂MePO₃, **II**, and SnPO₃CH₂COOH, **VII**) to 2D layers (i.e., Sn₂Cl₂(EtPO₃)EtPO₂OH, **III**, β -SnEtPO₃, **IV**, and SnMePO₃, **V**) to 3D frameworks (i.e., Sn₂(O₃P(CH₂)₂PO₃), **VI**), synthesized in the absence of structure-directing/charge-compensating agents. For the first time, a three-ring (3R) chain has been isolated. The existence of this chain

as a motif in structures reported here and in the literature underscores its role in higher dimensional materials. The origin of the 3R chain itself is also addressed below.

Syntheses

All syntheses were carried out hydrothermally and the final compositions are listed in Table 1. In a typical synthesis, tin(II) chloride was stirred in deionized water. The desired acid (phosphonic or phosphinic) was added and the mixture stirred until homogeneous. For the synthesis of **VIII**, ammonium chloride was also added. The gels were sealed in a 23-mL Teflon-lined stainless steel autoclave (Parr) and heated at 150–160 °C for 24–48 h. The products were filtered under vacuum, washed with minimal amounts of water, and dried at room temperature in air.

Single-Crystal X-ray Crystallography

A suitable single crystal of each compound was selected under a polarizing microscope and glued to a thin glass fiber with cyanoacrylate (Superglue) adhesive. Structure determination by X-ray diffraction was performed on a Siemens SMART-CCD diffractometer equipped with a normal focus, 2.4-kW sealed tube X-ray source (Mo K α radiation, $\lambda = 0.71073$ Å) operating at 45 kV and 40 mA. In each case, a hemisphere of intensity data was collected at room temperature in 1321 frames with ω scans (width 0.30° and exposure time of 10–20 s/frame). An empirical correction based on symmetry-equivalent reflections was applied using the SADABS program.¹⁴ The structure was solved by direct methods using SHELX-97 and difference Fourier syntheses.¹⁵ Full-matrix least-squares refinement against $|F^2|$ was carried out using the SHELXTL-PLUS package of programs.¹⁵ For **I** and **IV**–**VIII**, the complete data set was used for structure solution and refinement. For **II** and **III**, the first 606 frames were used to solve and refine the structure successfully to good *R* values since the use of merged data files resulted in relatively poor structural refinement due to decomposition of the crystals during the course of data collection. The last cycles of refinement included atomic positions for all atoms, anisotropic thermal parameters for non-hydrogen atoms, and isotropic thermal parameters for hydrogen atoms. Details of final refinement are presented in Tables 2 and 3. Fractional atomic coordinates and selected bond distances and angles are given in Tables 4–19.

Additional Details of the Structure Refinements. For **I**, H atoms could be located in the Fourier difference map. Bond distances for X–H (X = C, P) atom pairs are given in Table 5, in contrast with other structures throughout the article where H atom locations are placed using a riding model. The spheres representing the thermal motion of the H atoms (Figure 1) are much larger than those in the other representations of H

(10) (a) Murugavel, R.; Voight, A.; Walawalkar, M. G.; Roesky, H. W. *Chem. Rev.* **1996**, *96*, 2205. (b) Mason, M. R. *J. Cluster Sci.* **1997**, *36*, 239.

(11) Oliver, S.; Kuperman, A.; Ozin, G. A. *Angew. Chem., Int. Ed.* **1998**, *37*, 46.

(12) (a) Rao, C. N. R.; Natarajan, S.; Choudhury, A.; Neeraj, S.; Ayi, A. A. *Acc. Chem. Res.* **2001**, *34*, 80. (b) Ayi, A. A.; Choudhury, A.; Natarajan, S.; Neeraj, S.; Rao, C. N. R. *J. Mater. Chem.* **2001**, *11*, 1181.

(13) (a) Natarajan, S.; Attfield, M. P.; Cheetham, A. K. *Angew. Chem., Int. Ed. Engl.* **1997**, *36*, 978. (b) Natarajan, S.; Cheetham, A. K. *Chem. Commun.* **1997**, 1089. (c) Natarajan, S.; Cheetham, A. K. *J. Solid State Chem.* **1997**, *134*, 207. (d) Ayyappan, S.; Bu, X.; Cheetham, A. K.; Rao, C. N. R. *Chem. Mater.* **1998**, *10*, 3308.

(14) Sheldrick, G. M. *SADABS User Guide*; University of Göttingen: Göttingen, Germany, 1995.

(15) Sheldrick, G. M. *SHELXL-97, A program for crystal structure determination*; University of Göttingen: Göttingen, Germany, 1997.

Table 2

	I	II	III	IV
chemical formula	SnCl(HPhPO ₂)	(SnCl) ₂ MePO ₃	Sn ₂ Cl(EtPO ₃)EtPO ₂ OH	β -SnEtPO ₃
formula mass	295.25	402.33	489.95	226.74
system/space group	triclinic/ $\bar{P}\bar{1}$	triclinic/ $\bar{P}\bar{1}$	monoclinic/ $P2_1/m$	Cc
<i>a</i> (Å)	5.4767(6)	4.7275(17)	4.814(4)	4.6415(13)
<i>b</i> (Å)	8.8106(9)	6.152(2)	8.530(4)	18.695(5)
<i>c</i> (Å)	9.5219(10)	13.632(5)	15.214(8)	6.4964(18)
α (deg)	104.564(2)	81.299(7)	90	90
β (deg)	95.440(2)	89.052(7)	99.09(10)	99.907(4)
γ (deg)	99.349(2)	89.781(7)	90	90
volume (Å ³)	434.34(8)	391.8(3)	616.9(7)	555.3(3)
<i>Z</i> (formula units)	2	2	6	4
2 θ range (deg)	4.46–56.36	3.02–56.60	2.72–56.32	7.72–56.06
<i>R</i> (σ)/ <i>R</i> (int)	0.0306/0.0407	0.1061/0.1045	0.0818/0.1129	0.0378/0.0582
total reflections	4406	2280	1725	754
unique, all data	1943	1675	1302	587
unique, $F^2 > 4\sigma(F^2)$	1867	1164	921	571
R1/wR2, all data	0.0380/0.1002	0.1209/0.2444	0.0760/0.1543	0.0711/0.1830
R1/wR2, $F^2 > 4\sigma(F^2)$	0.0369/0.0987	0.0807/0.2233	0.0484/0.1207	0.0703/0.1818
<i>S</i> (Goof), all data	0.893	1.054	1.022	1.100
max/min res. dens. (e/Å ³)	−2.901/1.364	−2.913/6.353	−1.766/1.889	−3.913/2.276
parameters	124	83	90	61
structure type	open-chain wire	three-ring chains	three-ring layers	six-ring layers

Table 3

	V	VI	VII	VIII
chemical formula	SnMePO ₃	Sn ₂ (O ₃ P(CH ₂) ₂ PO ₃)	SnPO ₃ CH ₂ COOH	(NH ₄) ₂ Sn(O ₃ PCH ₂ PO ₃)
formula mass	212.72	423.42	256.73	326.76
system/space group	monoclinic/P2 ₁ /c	monoclinic/P2 ₁ /c	monoclinic/P2 ₁ /n	orthorhombic/Pbca
<i>a</i> (Å)	4.5998(7)	4.6435(6)	5.490(2)	10.3417(10)
<i>b</i> (Å)	15.430(2)	13.4512(16)	4.890(2)	10.0475(10)
<i>c</i> (Å)	6.5861(10)	6.4767(8)	21.884(9)	16.9927(17)
α (deg)	90	90	90	90
β (deg)	100.719(3)	100.258(2)	90.505(7)	90
γ (deg)	90	90	90	90
volume (Å ³)	459.30(12)	398.07(9)	587.4(4)	1765.7(3)
<i>Z</i> (formula units)	6	3	5	9
2 θ range (deg)	5.28–56.36	6.06–56.46	3.72–46.80	4.80–46.60
<i>R</i> (<i>o</i>)/ <i>R</i> (int)	0.0602/0.0734	0.0557/0.0735	0.0512/0.0709	0.0377/0.0752
total reflections	2620	2326	2460	7246
unique, all data	1034	901	858	1270
unique, $F^2 > 4\sigma(F^2)$	960	847	735	1119
R1/wR2, all data	0.0565/0.1511	0.0448/0.1100	0.0357/0.0723	0.0310/0.0734
R1/wR2, $F^2 > 4\sigma(F^2)$	0.0541/0.1501	0.0434/0.1087	0.0298/0.0703	0.0268/0.0714
<i>S</i> (GooF), all data	1.263	1.06	1.054	1.078
max/min res. dens. (e/Å ³)	-2.534/3.032	-1.617/1.739	-1.013/0.794	-0.519/0.769
parameters	56	56	91	92
structure type	six-ring layers	six-ring 3D	four-ring ladders	four-ring chains

atoms throughout the article since they were independently refined. For **III**, occupancies of C2 and C4 were refined independently and settled on 0.48 and 0.68, respectively, and then fixed at 0.5 during the last stages of refinement. The ADDSYM command in PLATON did not suggest space group changes.¹⁶ MISSYM suggested $C2/c$, but refinement could not proceed past $R1(F) = 0.32$ (where $F^2 > 4\sigma(F^2)$). After all atoms were located for **IV**, no additional atoms could be found in the difference Fourier map during the last stages of refinement. Thus, **IV** does not appear to have disordered ethyl groups, unlike **III** which also has [EtPO₃] units.

Structure I, $\text{SnCl}(\text{HPhPO}_2)$, Open-Chain Wires (i.e., No Rings)

The asymmetric unit of **I**, $\text{SnCl}(\text{HPhPO}_2)$, 295.25 g mol⁻¹, has 11 crystallographically independent non-hydrogen atoms (Figure 1). Atomic coordinates are found in Table 4, and bond distances and angles for

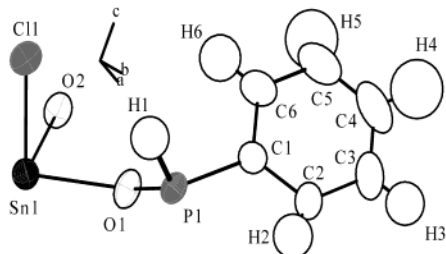


Figure 1. Asymmetric unit of **I** (thermal ellipsoids given at 50% probability). H atoms' ellipsoids are large due to refinement without the usual riding constraints.

selected atoms are given in Table 5. This tin(II) chloride phosphinate is made from $[\text{HPO}_2\text{Ph}]$ and $[\text{SnO}_2\text{ClE}]$ pseudo-tetrahedra (E = lone electron pair, occupying the fourth position of the $[\text{Sn}^{2+}]$ tetrahedron; alternatively, $[\text{SnO}_2\text{Cl}]$ is a trigonal pyramid). Bond distances and angles agree with those of related tin(II) phosphonates¹⁷ and phosphites¹⁸ (averages: $\text{Sn}-\text{O} = 2.124 \text{ \AA}$, $\text{Sn}-\text{Cl} = 2.528 \text{ \AA}$, $\text{P}-\text{O} = 1.516 \text{ \AA}$, $\text{P}-\text{C} = 1.783 \text{ \AA}$, $\text{P}-\text{H} =$

(16) Spek, A. L. *PLATON-94 (V-101094). A multipurpose crystallography tool*; University of Utrecht: Utrecht, The Netherlands, 1994.

Table 4. Atomic Coordinates and Isotropic Displacement Parameters for I

atom	<i>x</i>	<i>y</i>	<i>z</i>	<i>U</i> _{eq} ^a (Å ²)
Sn1	0.28133(3)	0.18460(2)	0.93271(2)	0.02907(14)
P1	0.85746(15)	0.35441(10)	1.13720(10)	0.0273(2)
Cl1	0.28300(16)	0.04495(10)	1.13438(10)	0.0369(2)
O1	0.6048(4)	0.3513(3)	1.0543(3)	0.0371(6)
O2	0.0720(5)	0.3437(3)	1.0484(3)	0.0352(5)
C1	0.9389(7)	0.5355(4)	1.2814(4)	0.0327(7)
H1	0.836(12)	0.226(8)	1.197(7)	0.063(16)
C2	1.1620(8)	0.6422(5)	1.2936(5)	0.0440(9)
H2	1.240(13)	0.584(8)	1.227(8)	0.065(17)
C3	1.2197(13)	0.7833(6)	1.4072(6)	0.0625(13)
H3	1.395(13)	0.830(8)	1.419(7)	0.063(17)
C4	1.0560(15)	0.8154(6)	1.5091(6)	0.0696(18)
H4	1.116(18)	0.901(13)	1.592(10)	0.12(3)
C5	0.8398(15)	0.7090(8)	1.4997(6)	0.0655(15)
H5	0.724(19)	0.722(14)	1.518(11)	0.12(4)
C6	0.7758(10)	0.5702(6)	1.3862(5)	0.0503(10)
H6	0.609(14)	0.504(9)	1.377(8)	0.072(19)

^a *U*_{eq} is defined as one-third of the trace of the orthogonalized *U*_{ij} tensor.

Table 5. Selected Bond Distances and Angles for I^a

moiety	dist. (Å)	moiety	dist. (Å)
Sn1–O2	2.116(2)	P1–O2 ^a	1.513(3)
Sn1–O1	2.132(3)	P1–O1	1.519(3)
Sn1–Cl1	2.5278(9)	P1–C1	1.783(4)
		P1–H1	1.39(7)
moiety	angle (deg)	moiety	angle (deg)
O2–Sn1–O1	86.19(11)	O1–P1–C1	108.16(15)
O2–Sn1–Cl1	89.78(8)	H1–P1–O2 ^a	107(3)
O1–Sn1–Cl1	88.84(8)	H1–P1–O1	109(3)
O2 ^a –P1–O1	116.33(17)	H1–P1–C1	109(3)
O2 ^a –P1–C1	107.92(16)		

Organic Group

moiety	dist. (Å)	moiety	dist. (Å)
C1–C2	1.391(6)	C2–H2	0.89(7)
C1–C6	1.411(6)	C3–H3	0.97(10)
C2–C3	1.395(7)	C4–H4	0.93(10)
C3–C4	1.391(10)	C5–H5	0.69(10)
C4–C5	1.366(11)	C6–H6	0.99(10)
C5–C6	1.382(8)		
moiety	angle (deg)	moiety	angle (deg)
C2–C1–C6	119.4(4)	C4–C3–C2	119.9(6)
C2–C1–P1	121.2(3)	C5–C4–C3	120.5(5)
C6–C1–P1	119.5(3)	C4–C5–C6	120.6(6)
C1–C2–C3	119.8(5)	C5–C6–C1	119.8(6)

^a Symmetry transformations used to generate equivalent atoms: *x* + 1, *y*, *z*.

1.39 Å; O–Sn–O = 86.2°, O–Sn–Cl = 89.3°, O–P–O = 116.3°, O–P–C = 108.0°, H–P–C = 109°, H–P–O = 108°. The P–O bond distances are shorter and the O–P–O bond angles larger than the corresponding distances and angles in phosphates (H and Ph ligands are less electronegative than O ligands). Bond distances and angles for the phenyl group lie within acceptable ranges (averages: C–C = 1.389 Å, C–H = 0.894 Å, C–C–C = 120.0°, C–C–P = 120.4°).

(17) (a) Zapf, P. J.; Rose, D. J.; Haushalter, R. C.; Zubieta, J. *J. Solid State Chem.* **1996**, *125*, 182. (b) Zapf, P. J.; Rose, D. J.; Haushalter, R. C.; Zubieta, J. *J. Solid State Chem.* **1997**, *132*, 438. (c) Adair, B.; Natarajan, S.; Cheetham, A. K. *J. Mater. Chem.* **1998**, *8*, 1477. (d) Lansky, D. E.; Zavalij, P. Y.; Oliver, S. R. *J. Acta Crystallogr. C* **2001**, *57*, 1051.

(18) (a) Yamaguchi, T.; Lindqvist, O. *Acta Crystallogr., Sect. B: Struct. Sci.* **1982**, *38*, 1441. (b) McDonald, R. C.; Eriks, K. *Inorg. Chem.* **1980**, *19*, 1237.

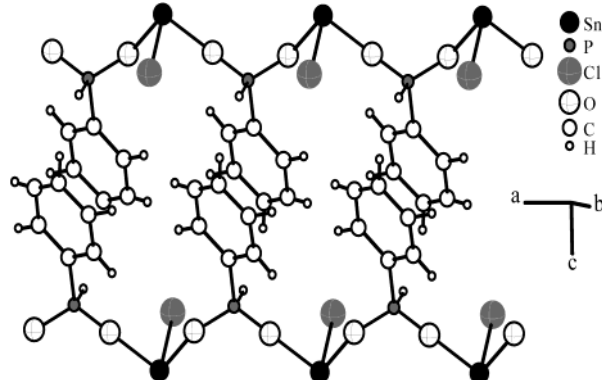


Figure 2. Alternating [SnO₂ClE] and [HPO₂Ph] pseudo-tetrahedra are connected in only two places each to form an open chain wire in **I**. Phenyl groups interact closely (e.g., C1–C5 = 3.617 Å, C5–C6 = 3.776 Å).

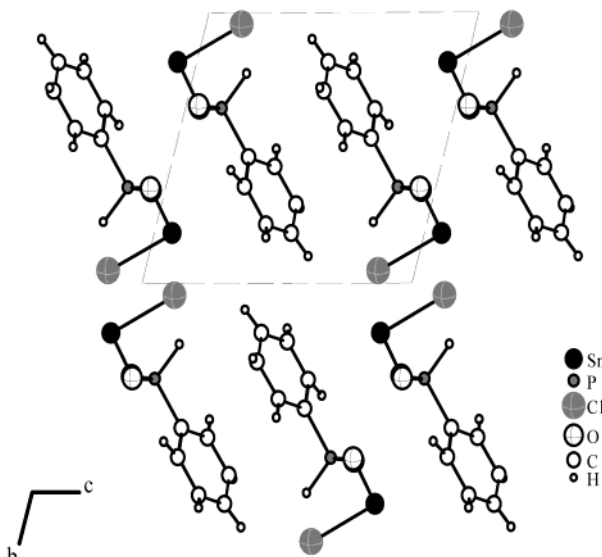


Figure 3. Packing of open-chain wires in **I**.

The [HPO₂Ph] and [SnClO₂E] pseudo-tetrahedra are both two-connected and form an open-chain “wire” where phenyl groups from adjacent wires are oriented such that they lie in the same plane and in close proximity with one another (Figure 2). The importance of a wire with respect to a possible formation mechanism is discussed later. However, **I** is also noteworthy for the fact that it is one of only a few known wires with M–O–P connectivity. The others (e.g., Zn(C₄N₂H₆)₂–(HPO₄)¹⁹, M[SnF(HPO₄)], (M = Na, NH₄)²⁰, CsSbF₃(H₂PO₄)²¹) indicate that open-chain wires are not limited to phosphinate systems but are also relevant to the metal phosphates.

Structure II, (SnCl)₂MePO₃, Isolated 3R Chains

The asymmetric unit of **II**, (SnCl)₂MePO₃, 402.33 g mol⁻¹, has 9 crystallographically independent non-hydrogen atoms (Figure 4). Atomic coordinates are found in Table 6, and bond distances and angles for

(19) Ayi, A. A.; Neeraj, S.; Choudhury, A.; Natarajan, S.; Rao, C. N. R. *J. Phys. Chem. Solid* **2001**, *62*, 1481.

(20) Kokunov, Y. V.; Detkov, D. G.; Gorbunova, Y. E.; Ershova, M.; Mikhailov, Y. N. *Russ. J. Inorg. Chem.* **2002**, *47*, 832.

(21) Davidovich, R. L.; Zemnukhova, L. A.; Fedorishcheva, G. A.; Kaidalova, T. A.; Ivanov, S. B. *Koord. Khim.* **1990**, *16*, 177.

Table 6. Atomic Coordinates and Isotropic Displacement Parameters for II

atom	<i>x</i>	<i>y</i>	<i>z</i>	<i>U</i> _{eq} ^a (Å ²)
Sn1	0.3044(3)	0.0540(3)	0.13442(12)	0.0282(5)
Sn2	0.2797(3)	-0.2526(3)	0.42970(11)	0.0242(5)
P1	0.8166(11)	-0.2594(9)	0.2602(4)	0.0235(12)
Cl1	0.2739(12)	-0.2435(10)	0.0278(4)	0.0313(12)
Cl2	0.2865(14)	0.1609(10)	0.3985(4)	0.0374(14)
O1	0.712(3)	-0.073(3)	0.1863(11)	0.025(3)
O2	0.694(4)	-0.279(3)	0.3626(12)	0.039(4)
O3	0.144(3)	-0.225(3)	0.2681(12)	0.034(4)
C1	0.759(5)	-0.506(4)	0.2156(17)	0.032(5)
H1	0.8072	-0.4886	0.1461	0.048
H2	0.5635	-0.5466	0.225	0.048
H3	0.875	-0.6193	0.251	0.048

^a *U*_{eq} is defined as one-third of the trace of the orthogonalized *U*_{ij} tensor.

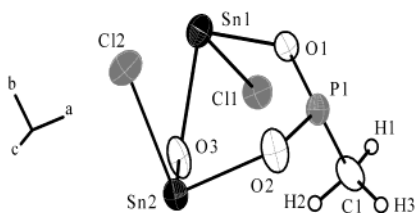


Figure 4. Asymmetric unit of **II** (thermal ellipsoids given at 50% probability).

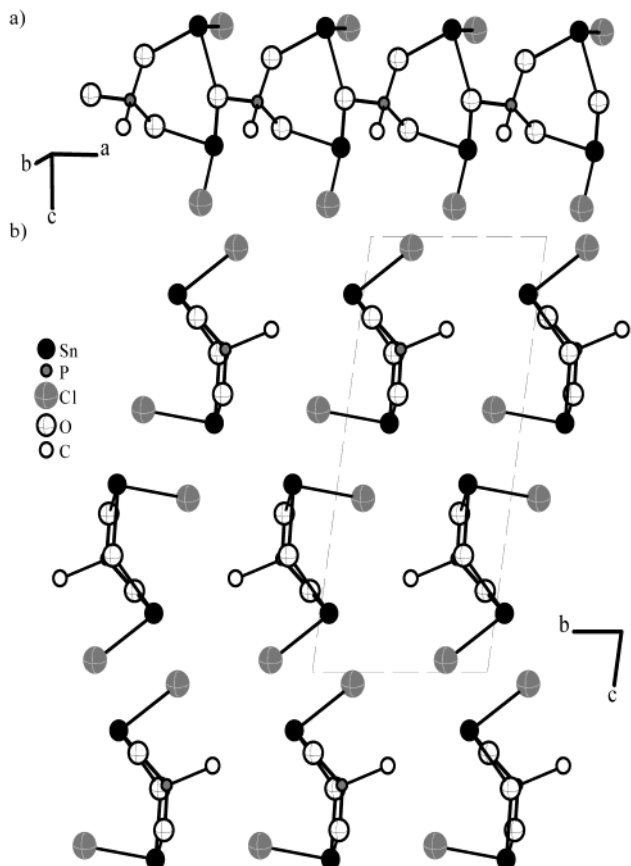


Figure 5. (a) Three-coordinated O links [SnO₂ClE] and [MePO₃] tetrahedra, giving a 3R chain; (b) packing arrangement in **II** is similar to that in **I** (Figure 3).

selected atoms are given in Table 7. This tin(II) chloride phosphonate has one crystallographically distinct [MePO₃] and two [SnO₂ClE] pseudo-tetrahedra. Bond distances and angles agree with those of related tin(II)

Table 7. Selected Bond Distances and Angles for II

moiety	dist. (Å)	moiety	dist. (Å)
Sn1–O1	2.167(14)	Sn2–Cl2	2.515(6)
Sn1–O3	2.419(18)	P1–O2	1.491(17)
Sn1–Cl1	2.509(6)	P1–O1	1.494(15)
Sn2–O2	2.164(17)	P1–O3 ^a	1.572(15)
Sn2–O3	2.286(16)	P1–C1	1.74(3)

moiety	angle (deg)	moiety	angle (deg)
O1–Sn1–O3	81.1(5)	O2–P1–O1	116.6(10)
O1–Sn1–Cl1	89.6(4)	O2–P1–O3 ^a	107.3(9)
O3–Sn1–Cl1	85.3(4)	O1–P1–O3 ^a	106.4(9)
O2–Sn2–O3	81.8(5)	O2–P1–C1	108.3(12)
O2–Sn2–Cl2	93.1(6)	O1–P1–C1	109.2(10)
O3–Sn2–Cl2	85.1(5)	O3 ^a –P1–C1	108.7(11)

^a Symmetry transformations used to generate equivalent atoms: *x* + 1, *y*, *z*.

phosphonates¹⁷ (averages: Sn–O = 2.259 Å, Sn–Cl = 2.512 Å, P–O = 1.519 Å, P–C = 1.74 Å; O–Sn–O = 81.5°, O–Sn–Cl = 88.3°, O–P–O = 110.1°, O–P–C = 108.7°). The P–O bond distances are shorter and O–P–O bond angles larger in this phosphonate than corresponding distances and angles in tin(II) phosphates,¹³ but the effect is not as pronounced as in the phosphinate (**I**).

The [SnO₂ClE] and [MePO₃] units make Sn₂P rings (Figure 5a). The O of the Sn–O–Sn linkage is three-coordinated, shared by a [MePO₃] group of another Sn₂P ring, linking the rings into a 3R chain (Figure 5). Such chains with M–O–P (M = metal) linkages play a role in many structures (see Discussion), but this is the first time such a chain has been isolated.

Structure III, Sn₂Cl(EtPO₃)EtPO₂OH, Layers with 3R Chains

The asymmetric unit of **III**, Sn₂Cl(EtPO₃)EtPO₂OH, 489.95 g mol⁻¹, has 12 crystallographically independent non-hydrogen atoms (Figure 6). Atomic coordinates are

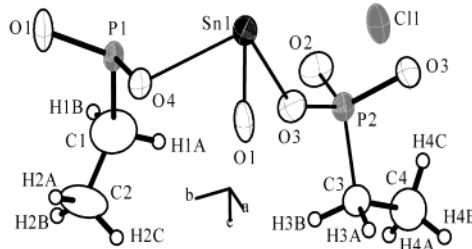


Figure 6. Asymmetric unit of **III** (thermal ellipsoids given at 50% probability).

found in Table 8, and bond distances and angles for selected atoms are given in Table 9. This tin(II) chloride phosphonate is made from [EtPO₃], [EtPO₂OH], and [SnO₃E] pseudo-tetrahedra. (Since the Sn–Cl distance is 2.981 Å, the Cl atom is not considered as part of the primary Sn(II) bonding sphere). Bond distances and angles agree with those of related tin(II) phosphonates¹⁷ (averages: Sn–O = 2.236 Å, nonterminal P–O = 1.523 Å, P–OH = 1.550 Å, P–C = 1.798 Å; O–Sn–O = 85.9°, O–P–O = 111.0°, O–P–C = 107.8°). Bond distances and angles for the ethyl group lie within acceptable ranges, though the C1–C2 distance (1.40(3) Å) is

Table 8. Atomic Coordinates and Isotropic Displacement Parameters for III

atom	<i>x</i>	<i>y</i>	<i>z</i>	<i>U</i> _{eq} ^a (Å ²)
Sn1	0.29056(13)	0.00936(8)	0.60835(4)	0.0247(3)
Cl1	0.6700(8)	-0.25	0.5710(3)	0.0352(9)
P1	0.8387(7)	0.25	0.6916(2)	0.0211(8)
P2	1.2392(7)	-0.25	0.7800(2)	0.0211(7)
O1	0.6984(14)	0.1010(8)	0.6525(6)	0.038(2)
O2	0.919(2)	-0.25	0.7841(8)	0.040(3)
O3	1.3226(15)	-0.1015(9)	0.7375(5)	0.0331(17)
O4	1.1519(17)	0.25	0.6738(6)	0.025(2)
C1	0.829(5)	0.25	0.8100(13)	0.072(7)
H1A ^b	0.8898	0.3534	0.8315	0.108
H1B ^b	0.6327	0.2409	0.8167	0.108
C2 ^b	0.976(6)	0.143(4)	0.8691(17)	0.061(8)
H2A ^b	1.0721	0.0691	0.8367	0.092
H2B ^b	0.8466	0.0875	0.8999	0.092
H2C ^b	1.1109	0.1974	0.9114	0.092
C3	0.613(3)	0.25	1.1045(10)	0.032(3)
H3A ^b	0.4102	0.2579	1.0993	0.048
H3B ^b	0.6789	0.3425	1.0769	0.048
C4 ^b	0.683(6)	0.108(3)	1.0540(18)	0.058(7)
H4A ^b	0.8549	0.0626	1.0836	0.087
H4B ^b	0.7053	0.1384	0.9947	0.087
H4C ^b	0.5336	0.0331	1.0514	0.087

^a *U*_{eq} is defined as one-third of the trace of the orthogonalized *U*_{ij} tensor. ^b Atom not on special positions with occupancy of 0.5.

Table 9. Selected Bond Distances and Angles for III

moiety	dist. (Å)	moiety	dist. (Å)
Sn1–O1	2.122(7)	P1–C1	1.808(19)
Sn1–O3 ^a	2.165(7)	P2–O3	1.505(7)
Sn1–O4 ^a	2.421(5)	P2–O2	1.550(11)
P1–O1	1.516(7)	P2–C3 ^d	1.788(16)
P1–O4	1.573(9)		

moiety	angle (deg)	moiety	angle (deg)
O1–Sn1–O3 ^a	86.8(3)	O4–P1–C1	110.4(9)
O1–Sn1–O4 ^a	81.9(3)	O3–P2–O3 ^c	114.6(6)
O3 ^a –Sn1–O4 ^a	88.9(3)	O3–P2–O2	110.6(4)
O1–P1–O1 ^b	113.9(6)	O3–P2–C3 ^d	109.3(4)
O1–P1–O4	108.2(3)	O2–P2–C3 ^d	101.7(7)
O1–P1–C1	108.1(5)		

Organic Groups

moiety	dist. (Å)	moiety	angle (deg)
C1–C2	1.40(3)	C2–C1–P1	123.3(15)
C3–C4	1.50(3)	C4–C3–P2 ^d	114.6(13)

^{a–d} Symmetry transformations used to generate equivalent atoms: ^a *x* – 1, *y*, *z*; ^b *x*, *y* + 1/2, *z*; ^c *x*, *y* – 1/2, *z*; ^d *x* + 2, *y*, *z* + 2.

somewhat shorter than expected (averages: C–C = 1.45 Å; C–C–P = 119.0°). The [CH₃] parts (C2, C4) of the ethyl groups lie on two sites with 0.5 occupancy.

The overall structure of **III** is like that of Sn₂(C₂O₄)₂MePO₃,^{17c} where chains based on Sn₂P rings are linked together to form layers. Some differences are as follows: (1) in **III**, chains are linked through a [EtPO₂–OH] (Figure 7) rather than a [C₂O₄] group; (2) in **III**, the orientation of the Sn₂P rings along the [100] direction is the same for adjacent chains, instead of alternating; (3) in **III**, P–C bonds point along the [001] direction for one layer and the [001] direction for neighboring layers (Figure 8), whereas in Sn₂(C₂O₄)₂MePO₃, P–C bonds of one chain point along [001] and along [001] for adjacent chains. Thus, a family of these layered materials could exist, where chains are connected in various orientations.

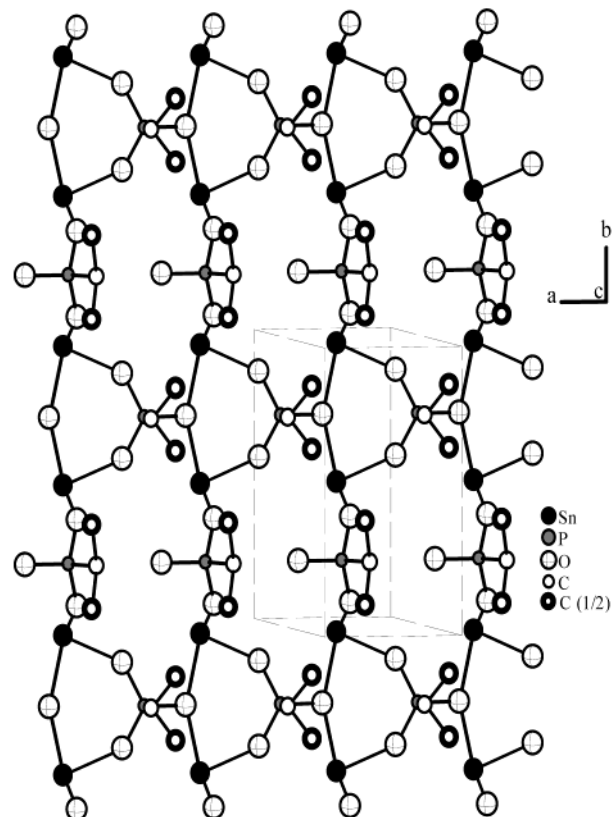


Figure 7. Phosphonate groups connect 3R chains (like those of **II**) to form layers in **III**. Partial occupancies of C2 and C4 are depicted by heavy black circles.

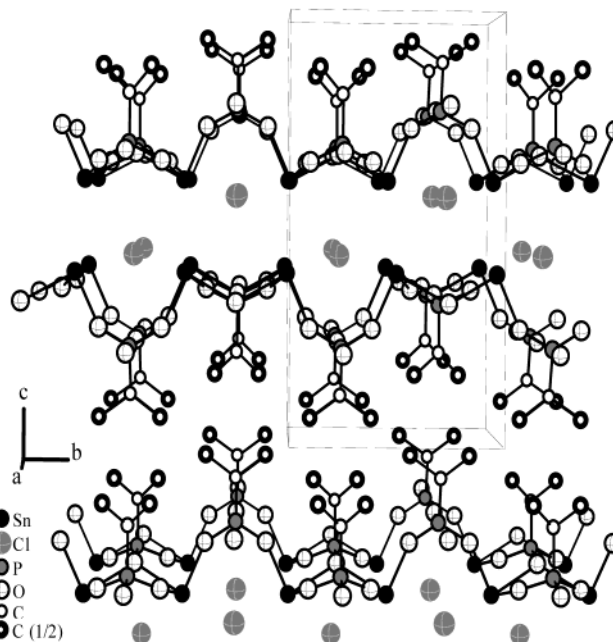


Figure 8. Cl[–] anions sit between layers of **III**, providing charge compensation.

Structures IV and V, β -SnEtPO₃ and SnMePO₃, Layers with 3R Chains

The asymmetric unit of **IV**, β -SnEtPO₃, 226.74 g mol^{–1}, has 7 crystallographically independent non-hydrogen atoms (Figure 9). Atomic coordinates are found in Table 10, and bond distances and angles for

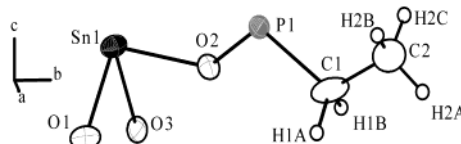


Figure 9. Asymmetric unit of **IV** (thermal ellipsoids given at 50% probability).

Table 10. Atomic Coordinates and Isotropic Displacement Parameters for IV

atom	<i>x</i>	<i>y</i>	<i>z</i>	<i>U</i> _{eq} ^a (Å ²)
Sn1	-0.4168(4)	0.43083(6)	0.3940(4)	0.0211(5)
P1	0.0178(11)	0.4236(3)	1.0205(8)	0.0167(11)
O1	-0.123(3)	0.3905(9)	1.195(2)	0.027(3)
O2	-0.185(3)	0.4726(7)	0.8755(19)	0.020(3)
O3	0.307(3)	0.4651(8)	1.1128(18)	0.024(3)
C1	-0.390(5)	0.1513(13)	1.361(3)	0.039(7)
H1A	-0.269	0.1334	1.2641	0.058
H1B	-0.5686	0.1698	1.2789	0.058
C2	-0.232(5)	0.2111(13)	1.483(3)	0.061(10)
H2A	-0.1806	0.2466	1.3888	0.092
H2B	-0.0583	0.1931	1.5687	0.092
H2C	-0.3568	0.2322	1.57	0.092

^a *U*_{eq} is defined as one-third of the trace of the orthogonalized \mathbf{U}_{ij} tensor.

Table 11. Selected Bond Distances and Angles for IV

moiety	dist. (Å)	moiety	dist. (Å)
Sn1–O2 ^a	2.116(14)	P1–O2	1.519(13)
Sn1–O3 ^b	2.140(13)	P1–O1	1.536(14)
Sn1–O1 ^c	2.167(13)	P1–O3	1.579(14)
		P1–C1 ^d	1.837(19)
moiety	angle (deg)	moiety	angle (deg)
O2 ^a –Sn1–O3 ^b	86.1(5)	O1–P1–O3	111.1(8)
O2 ^a –Sn1–O1 ^c	83.4(6)	O2–P1–C1 ^d	106.9(9)
O3 ^b –Sn1–O1 ^c	86.6(5)	O1–P1–C1 ^d	106.4(10)
O2–P1–O1	113.8(8)	O3–P1–C1 ^d	108.8(10)
O2–P1–O3	109.6(8)		

Organic Group

moiety	dist. (Å)	moiety	angle (deg)
C1–C2	1.4872	C2–C1–P1 ^e	114.4(7)

^{a–e} Symmetry transformations used to generate equivalent atoms: ^a $x, -y + 1, z - 1/2$; ^b $x - 1, y, z - 1$; ^c $x, y, z - 1$; ^d $x + 1/2, -y + 1/2, z - 1/2$; ^e $x - 1/2, -y + 1/2, z + 1/2$.

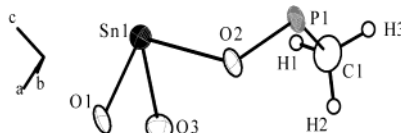


Figure 10. Asymmetric unit of **V** (thermal ellipsoids given at 50% probability).

selected atoms are given in Table 11. This tin(II) phosphonate has $[\text{EtPO}_3]$ and $[\text{SnO}_3\text{E}]$ pseudo-tetrahedra. Bond distances and angles agree with those of related tin(II) phosphonates¹⁷ (averages: Sn–O = 2.141 Å, P–O = 1.545 Å, P–C = 1.837 Å, C–C = 1.487 Å; O–Sn–O = 85.4°, O–P–O = 111.5°, O–P–C = 107.4°, C–C–P = 114.4°).

The asymmetric unit of **V**, SnMePO_3 , $212.72 \text{ g mol}^{-1}$, has 6 crystallographically independent non-hydrogen atoms (Figure 10). Atomic coordinates are found in Table 12, and bond distances and angles for selected atoms are given in Table 13. This tin(II) phosphonate has $[\text{MePO}_3]$ and $[\text{SnO}_3\text{E}]$ pseudo-tetrahedra. Bond distances and angles agree with those of related tin(II)

Table 12. Atomic Coordinates and Isotropic Displacement Parameters for V

atom	<i>x</i>	<i>y</i>	<i>z</i>	<i>U</i> _{eq} ^a (Å ²)
Sn1	0.44562(16)	0.66485(5)	0.72978(11)	0.0211(3)
P1	0.8720(5)	0.65932(17)	0.3614(4)	0.0174(5)
O1	0.6629(16)	0.7175(5)	0.2144(12)	0.0238(16)
O2	1.1483(15)	0.7107(5)	0.4623(12)	0.0239(16)
O3	0.7267(17)	0.6167(5)	0.5265(12)	0.0258(16)
C1	0.990(3)	0.5745(8)	0.210(2)	0.033(3)
H1	1.1164	0.5353	0.2994	0.05
H2	1.0961	0.599	0.1118	0.05
H3	0.82	0.5436	0.1388	0.05

^a *U*_{eq} is defined as one-third of the trace of the orthogonalized \mathbf{U}_{ij} tensor.

Table 13. Selected Bond Distances and Angles for V

moiety	dist. (Å)	moiety	dist. (Å)
Sn1–O1 ^a	2.084(8)	P1–O1	1.523(8)
Sn1–O2 ^b	2.140(7)	P1–O3	1.527(8)
Sn1–O3	2.159(8)	P1–O2	1.540(8)
		P1–C1	1.788(13)

moiety	angle (deg)	moiety	angle (deg)
O1 ^a –Sn1–O2 ^b	84.9(3)	O3–P1–O2	110.5(5)
O1 ^a –Sn1–O3	85.5(3)	O1–P1–C1	107.4(5)
O2 ^b –Sn1–O3	88.2(3)	O3–P1–C1	107.4(6)
O1–P1–O3	113.4(5)	O2–P1–C1	107.8(6)
O1–P1–O2	110.1(4)		

^{a–b} Symmetry transformations used to generate equivalent atoms: ^a $x, -y + 3/2, z + 1/2$; ^b $x - 1, y, z$.

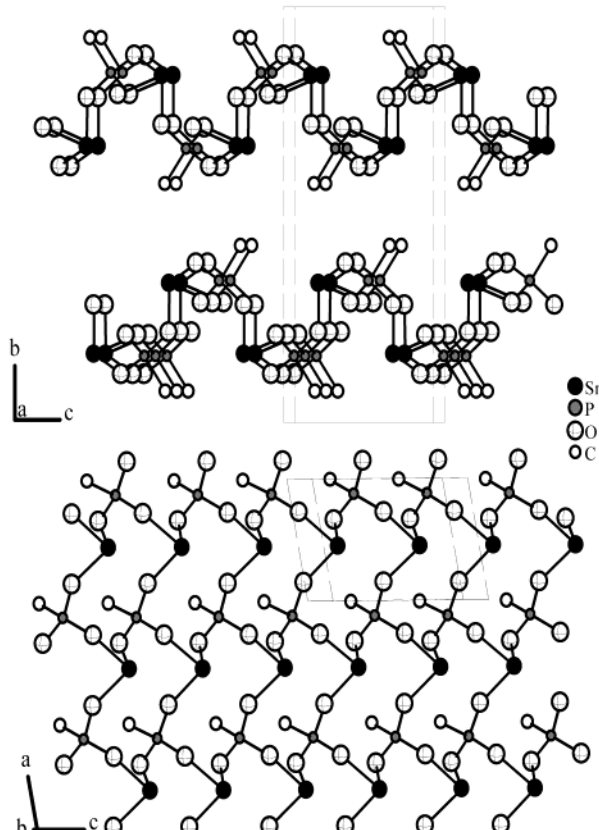


Figure 11. **V** (top) and **IV** (not shown) have Sn_3P_3 6R layers; **IV** has a longer *b* axis than **V** to accommodate $[\text{EtPO}_3]$ groups.

phosphonates¹⁷ (averages: Sn–O = 2.128 Å, P–O = 1.530 Å, P–C = 1.788 Å; O–Sn–O = 86.2°, O–P–O = 111.3°, O–P–C = 107.5°).

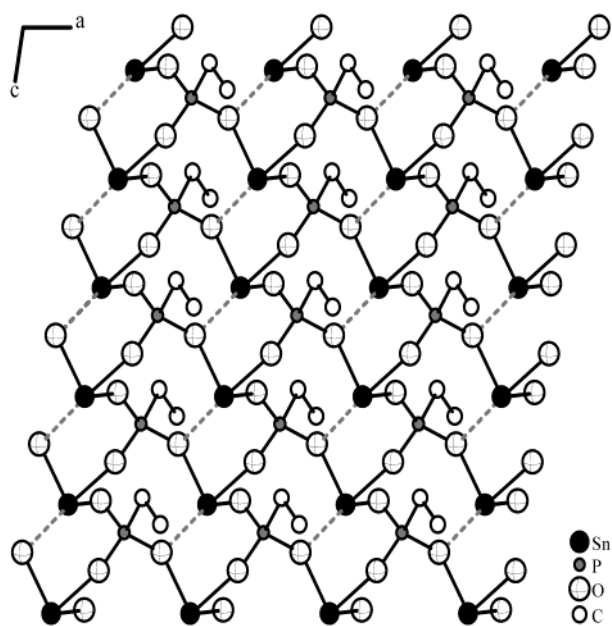


Figure 12. Layers of **IV** (nearly identical to those of **V**, SnPhPO_3 , SnHPO_3 , and SnPO_3F) contain 3Rs when secondary Sn–O bonds are considered (dashed). Compare with Figure 7.

IV and **V** have nearly identical layered structures, made from Sn_3P_3 six-rings (6Rs) (**IV** has an ethyl group while **V** has a methyl group coordinated to the phosphorus, Figure 11). SnPhPO_3 ,^{17d} SnHPO_3 ,^{18b} and SnPO_3F ²² have the same layers and all five materials share similar unit cell parameters (the differences coming from the ways that the layers are stacked to accommodate the phosphate/phosphonate/phosphite groups). Alternatively, if secondary Sn–O interactions are considered, the relationship between Sn_3P_3 6R layers and Sn_2P 3R chains is evident. Figures 7 (**III**) and 12 (**IV**) show views of the structures containing the same number of Sn, P, and O atoms. The difference is that **IV** has more bonds: consider the chains running in the [100] direction in Figure 7 and locate the equivalents in Figure 12; in **IV**, the P–OH is replaced by an O that links to the Sn of an adjacent chain through a primary bond (2.140 Å) and the Sn of another chain through a secondary bond (2.841 Å). The number of bonds to Sn stays the same in **III** and **IV**, so one primary bond of the original 3R chain is lengthened into a secondary bond and the 3Rs disappear, giving 6Rs when only primary bonds are considered (as depicted in Figure 11 for **V**).

Structure VI, $\text{Sn}_2(\text{O}_3\text{P}(\text{CH}_2)_2\text{PO}_3)$, A Diphosphonate Three-Dimensional Framework

The asymmetric unit of **VI**, $\text{Sn}_2(\text{O}_3\text{P}(\text{CH}_2)_2\text{PO}_3)$, 423.42 g mol⁻¹, has 6 crystallographically independent non-hydrogen atoms (Figure 13). Atomic coordinates are found in Table 14, and bond distances and angles for selected atoms are found in Table 15. This tin(II) diphosphonate has $[\text{SnO}_3\text{E}]$ and $[-\text{CH}_2\text{PO}_3]$ pseudo-tetrahedra where the $[-\text{CH}_2\text{PO}_3]$ units are linked

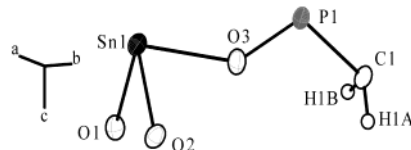


Figure 13. Asymmetric view of **VI** (thermal ellipsoids given at 50% probability).

Table 14. Atomic Coordinates and Isotropic Displacement Parameters for VI

atom	<i>x</i>	<i>y</i>	<i>z</i>	<i>U</i> _{eq} ^a (Å ²)
Sn1	0.10089(6)	0.65445(2)	0.52528(5)	0.0158(3)
P1	-0.3299(2)	0.85629(8)	0.4008(2)	0.0127(3)
O1	0.3843(6)	0.6997(2)	0.8101(5)	0.0178(7)
O2	-0.1937(7)	0.5982(2)	0.7236(5)	0.0180(7)
O3	-0.1237(6)	0.7887(2)	0.5495(5)	0.0181(7)
C1	-0.4138(10)	0.9584(3)	0.5621(8)	0.0184(10)
H1A	-0.5253	0.9331	0.664	0.022
H1B	-0.2321	0.9854	0.6388	0.022

^a *U*_{eq} is defined as one-third of the trace of the orthogonalized *U*_{ij} tensor.

Table 15. Selected Bond Distances and Angles for VI

moiety	dist. (Å)	moiety	dist. (Å)
Sn1–O3	2.105(3)	P1–O3	1.531(3)
Sn1–O1	2.154(3)	P1–O2 ^a	1.534(3)
Sn1–O2	2.172(3)	P1–O1 ^b	1.548(3)
		P1–C1	1.809(5)
moiety	angle (deg)	moiety	angle (deg)
O3–Sn1–O1	85.93(12)	O2 ^a –P1–O1 ^b	110.52(18)
O3–Sn1–O2	83.25(12)	O3–P1–C1	105.2(2)
O1–Sn1–O2	86.86(12)	O2–P1–C1	106.8(2)
O3–P1–O2 ^a	114.40(18)	O1–P1–C1	109.28(19)
O3–P1–O1 ^b	110.34(18)		

^{a–b} Symmetry transformations used to generate equivalent atoms: ^a *x*, $-y + \frac{3}{2}$, $z - \frac{1}{2}$; ^b *x* – 1, $-y + \frac{3}{2}$, $z - \frac{1}{2}$.

together to give an ethylenediphosphonate group. Bond distances and angles agree with those of related tin(II) phosphonates¹⁷ (averages: Sn–O = 2.144 Å, P–O = 1.538 Å, P–C = 1.809 Å; O–Sn–O = 85.3°, O–P–O = 111.8°, O–P–C = 107.1°).

The framework of **VI** has the same 6R layers as **IV** and **V**, joined through the diphosphonate group and creating Sn_4P_6 ten-rings (10Rs) (Figure 14). The layers, lying parallel to the *ac* plane, are stacked nearly identically in **III** and **IV** but are shifted in **VI** to allow the diphosphonate group to connect the layers (Figures 11 and 14). Cell parameters defining the *ac* plane are nearly the same for **IV**, **V**, and **VI** (Tables 2 and 3). It should be possible to make other members of the $\text{Sn}_2(\text{O}_3\text{RPO}_3)$ family, where layers are joined through bridging organic groups. Indeed, a number of zirconium diphosphonates were made based on this strategy.²³

The 10Rs in **VI** might be expected to be larger than 10Rs found in zeolites since (i) Sn–O bonds (~2.1 Å) are longer than Al–O (~1.7 Å) and Si–O bonds (~1.6 Å) and (ii) some phosphorus atoms are connected through bridging ethylene groups, rather than much shorter P–O–M linkages. However, in **VI**, the openings do not take the shape of a circle or ellipse as in most zeolites, but rather a more tortuous opening (Figure 14). In addition, the lone electron pairs reside in the

(22) Berndt, A. F. *Acta Crystallogr., Sect. B: Struct. Sci.* **1974**, *30*, 529.

(23) Clearfield, A. *Curr. Opin. Solid State Mater. Sci.* **1996**, *1*, 268 and references therein.

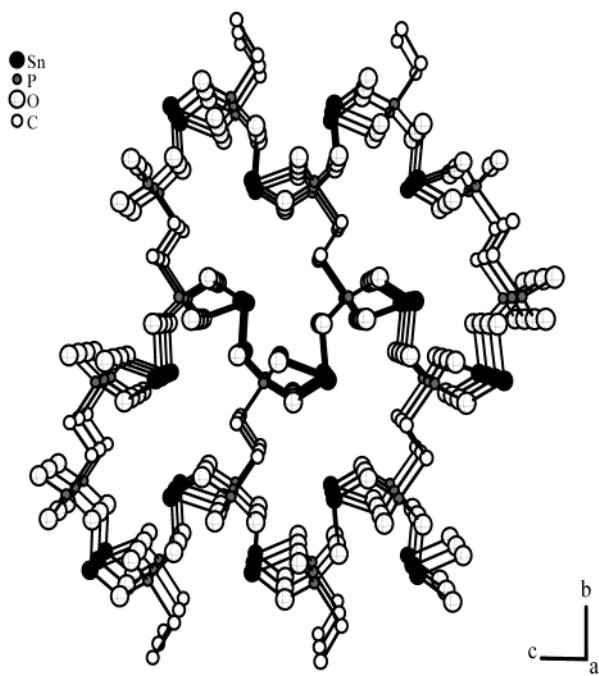


Figure 14. 6R layers like those in **IV** and **V** are connected through diphosphonate groups to form the **VI** framework. Compare with Figure 11.

channels and eliminate potential porosity. **VI** shows no significant adsorption of N_2 at 77 K, displaying a type II isotherm (associated with a nonporous material).²⁴

Structure VII, $SnPO_3CH_2COOH$, 4R Ladders

The asymmetric unit of **VII**, 256.73 g mol⁻¹, has 9 crystallographically independent non-hydrogen atoms (Figure 15). Atomic coordinates are found in Table 16,

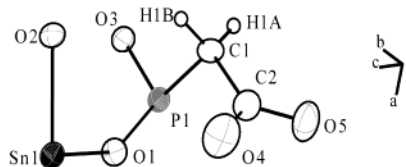


Figure 15. Asymmetric view of **VII** (thermal ellipsoids given at 50% probability).

and bond distances and angles for selected atoms are found in Table 17. This tin(II) phosphonocarboxylate has one crystallographically distinct $[SnO_3E]$ and one unique $[PO_3CH_2COOH]$ pseudo-tetrahedra. The C1–C2 distance is 1.500 Å, C2–O4 is 1.216(9) Å, and C2–O5 is 1.306(8) Å, whereas O4–C2–C5 = 124.0(7)°, all consistent with an acetate group (with a C=O double bond and C–OH bond). The hydrogen of the hydroxyl group could not be located in the Fourier difference map. Other bond distances and angles agree with those of related tin(II) phosphonates¹⁷ (averages: Sn–O = 2.217 Å, P–O = 1.526 Å; O–Sn–O = 87.9°, O–P–O = 111.8°, O–P–C = 107.1°).

In **VII**, Sn_2P_2 4Rs share edges to make ladders (Figure 16). Although this is the only tin(II) structure

Table 16. Atomic Coordinates and Isotropic Displacement Parameters for VII

atom	<i>x</i>	<i>y</i>	<i>z</i>	<i>U</i> _{eq} ^a (Å ²)
Sn1	0.81532(8)	0.21899(8)	0.932687(19)	0.0203(3)
P1	0.4054(3)	-0.3090(3)	0.92654(7)	0.0183(4)
O1	0.6469(7)	-0.1641(8)	0.93849(19)	0.0247(10)
O2	0.4522(7)	0.3834(8)	0.92597(18)	0.0229(10)
O3	0.1995(8)	-0.2334(8)	0.96991(19)	0.0239(11)
C1	0.2997(13)	-0.2097(14)	0.8510(3)	0.0228(15)
H1A	0.173(12)	-0.310(12)	0.849(3)	0.020(18)
H1B	0.270(13)	-0.005(16)	0.851(3)	0.05(2)
C2	0.4922(15)	-0.2690(14)	0.8047(3)	0.0286(17)
O4	0.6655(10)	-0.1186(13)	0.7969(2)	0.0520(15)
O5	0.4655(9)	-0.5061(11)	0.7779(2)	0.0458(14)

^a *U*_{eq} is defined as one-third of the trace of the orthogonalized U_{ij} tensor.

Table 17. Selected Bond Distances and Angles for VII

moiety	dist. (Å)	moiety	dist. (Å)
Sn1–O1	2.093(4)	P1–O3	1.528(5)
Sn1–O3 ^a	2.135(4)	P1–C1	1.813(7)
Sn1–O2	2.153(4)	C1–C2	1.500(10)
P1–O1	1.524(5)	C2–O4	1.216(9)
P1–O2 ^b	1.526(4)	C2–O5	1.306(8)

moiety	angle (deg)	moiety	angle (deg)
O1–Sn1–O3 ^a	87.04(16)	O2 ^b –P1–C1	108.0(3)
O1–Sn1–O2	85.93(16)	O3–P1–C1	105.6(3)
O3 ^a –Sn1–O2	90.71(17)	C2–C1–P1	110.1(5)
O1–P1–O2 ^b	108.3(2)	O4–C2–O5	124.0(7)
O1–P1–O3	115.4(2)	O4–C2–C1	122.4(7)
O2 ^b –P1–O3	111.7(2)	O5–C2–C1	113.4(7)
O1–P1–C1	107.6(3)		

^{a–b} Symmetry transformations used to generate equivalent atoms: ^a $-x + 1, -y, -z + 2$; ^b $x, y - 1, z$.

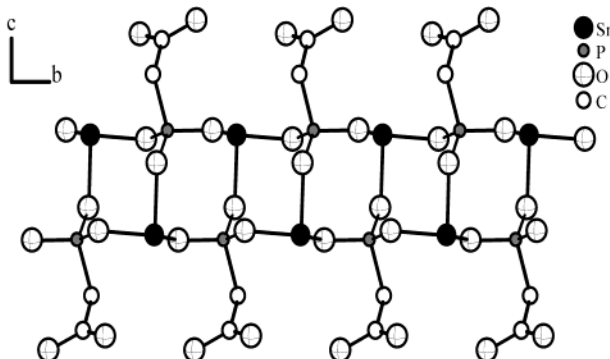


Figure 16. 4R ladders make up the structure of **VII**.

with edge-sharing 4Rs reported in this article, this kind of ladder is very common, found in numerous metal phosphates. In fact, the tin(II) phosphate analogue, $[C_6N_2H_{18}](SnPO_4)_2$, was recently reported, where isolated ladders are separated by organic cations.²⁵

Structure VIII, $(NH_4)_2Sn(O_3PCH_2PO_3)$, 4R Chains

The asymmetric unit of **VIII**, 326.76 g mol⁻¹, has 12 crystallographically independent non-hydrogen atoms (Figure 17). Atomic coordinates are found in Table 18, and bond distances and angles for selected atoms are found in Table 19. This is the first example in this article where the $[Sn^{2+}]$ coordination sphere resembles

(24) Sing, K. S. W.; Everett, D. H.; Haul, R. A. W.; Moscou, L.; Pierotti, R. A.; Rouquerol, J.; Siemieniewska, T. *Pure Appl. Chem.* **1985**, *57*, 603.

(25) Ayyappan, S.; Bu, X.; Cheetham, A. K.; Natarajan, S.; Rao, C. N. R.; *Chem. Commun.* **1998**, 2181.

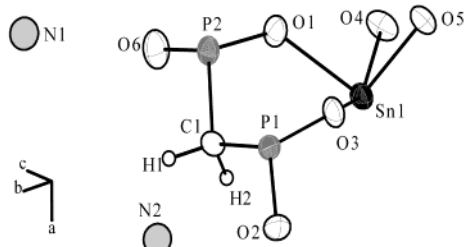


Figure 17. Asymmetric view of **VIII** (thermal ellipsoids given at 50% probability).

Table 18. Atomic Coordinates and Isotropic Displacement Parameters for **VIII**

atom	<i>x</i>	<i>y</i>	<i>z</i>	<i>U</i> _{eq} ^a (Å ²)
Sn1	0.89186(3)	0.00990(3)	0.402671(19)	0.0228(2)
P1	0.87694(11)	0.34435(11)	0.34227(7)	0.0195(3)
P2	0.78732(12)	0.27021(11)	0.50358(7)	0.0219(3)
O1	0.7784(3)	0.1220(3)	0.48156(18)	0.0293(8)
O2	0.9912(3)	0.3956(3)	0.29472(19)	0.0311(8)
O3	0.83630(13)	0.20421(14)	0.31994(8)	0.0270(7)
O4	0.83789(13)	-0.16007(14)	0.48005(8)	0.0314(8)
O5	0.73593(13)	-0.05575(14)	0.33263(8)	0.0265(7)
O6	0.81960(13)	0.28471(14)	0.58942(8)	0.0379(9)
N1	0.76102(13)	0.53136(14)	0.66090(8)	0.0357(11)
N2	0.94970(13)	0.68551(14)	0.31529(8)	0.0348(10)
C1	0.91589(13)	0.34531(14)	0.44601(8)	0.0228(10)
H1	0.9292	0.4363	0.4633	0.027
H2	0.9956	0.2966	0.4545	0.027

^a *U*_{eq} is defined as one-third of the trace of the orthogonalized *U*_{ij} tensor.

Table 19. Selected Bond Distances and Angles for **VIII**

moiety	dist. (Å)	moiety	dist. (Å)
Sn1–O1	2.107(3)	P1–O5 ^a	1.5482(17)
Sn1–O5	2.1100(14)	P1–C1	1.8082(17)
Sn1–O4	2.2265(14)	P2–O6	1.5035(17)
Sn1–O3	2.4735(14)	P2–O4 ^a	1.5255(18)
P1–O3	1.5177(18)	P2–O1	1.538(3)
P1–O2	1.521(3)	P2–C1	1.8150(18)
moiety	angle (deg)	moiety	angle (deg)
O1–Sn1–O5	95.76(10)	O3–P1–C1	108.08(10)
O1–Sn1–O4	83.95(9)	O2–P1–C1	110.06(15)
O5–Sn1–O4	84.4	O5 ^a –P1–C1	105.52(10)
O1–Sn1–O3	79.08(9)	O6–P2–O4 ^a	113.47(11)
O5–Sn1–O3	75.4	O6–P2–O1	110.06(15)
O4–Sn1–O3	151.99(7)	O4 ^a –P2–O1	109.27(16)
O3–P1–O2	113.37(15)	O6–P2–C1	108.66(10)
O3–P1–O5 ^a	111.48(8)	O4 ^a –P2–C1	106.84(11)
O2–P1–O5 ^a	108.03(15)	O1–P2–C1	108.37(14)

^a Symmetry transformations used to generate equivalent atoms: $-x + \frac{3}{2}, y + \frac{1}{2}, z$.

an [Sb³⁺] moiety with four-connected [SnO₄E] trigonal bipyramids, although this coordination is found in other tin(II) phosphates and phosphonates. Two crystallographically distinct $[-\text{CH}_2\text{PO}_3]$ tetrahedra have two bridging O²⁻ anions and a terminal P=O group and are linked together through the methylene group. Bond distances and angles agree with those of related tin(II) phosphonates¹⁷ (averages: Sn–O = 2.220 Å, P=O = 1.513 Å, nonterminal P–O = 1.526 Å, P–C = 1.812 Å; adjacent O–Sn–O = 83.7°, O–P–O = 110.9°, O–P–C = 107.9°). Charge compensation is provided by two crystallographically distinct NH₄⁺ cations. Each N has four O neighbors where the length of the N–O distance is less than 3.00 Å, averaging 2.87 Å (2.77–2.94 Å) for N1 and 2.93 Å (2.89–2.97 Å) for N2.

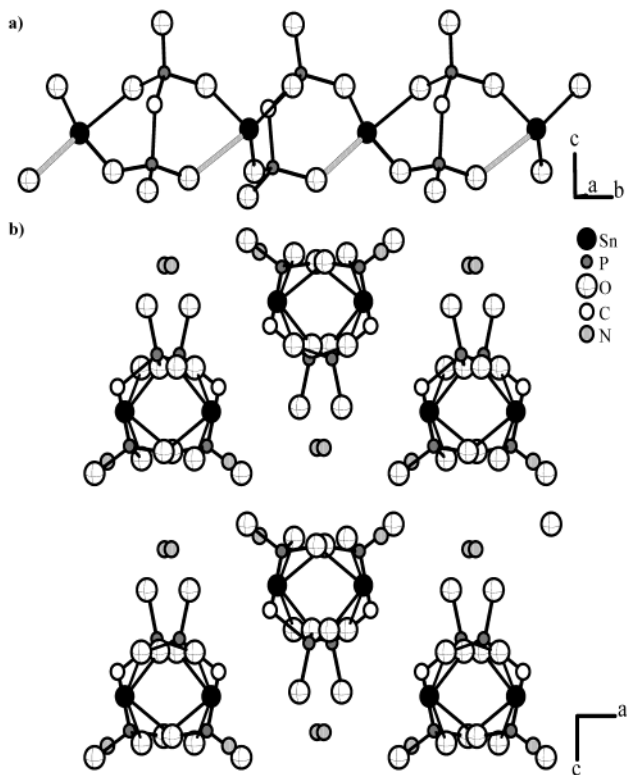


Figure 18. (a) 4R chains of **VIII** are nearly identical to those of (1) $\text{Sn}(\text{HO}_3\text{PCH}_2\text{PO}_3\text{OH}) \cdot \text{H}_2\text{O}$ (except the Sn–O bond shown in gray (2.474 Å) is longer and terminal P=O bonds are replaced by P–OH) and (2) $(\text{NH}_4)_2\text{Sn}(\text{HPO}_3)_2$ (except the P–CH₂ bonds are replaced by P–H bonds and the bond in gray is longer (2.696 Å)). (b) The chains are surrounded by NH₄⁺ charge-compensating cations.

Sn₂P₂ 4Rs share Sn sites to make chains (Figure 18a). The entire P–CH₂–P group belongs to one Sn₂P₂ ring, cutting the ring in half to make two SnP₂ 3Rs. **VIII** closely resembles two other structures, $\text{Sn}(\text{HO}_3\text{PCH}_2\text{PO}_3\text{H}) \cdot \text{H}_2\text{O}$ ^{17a} and $(\text{NH}_4)_2\text{Sn}(\text{HPO}_3)_2$.^{18a} The latter is a phosphite with P–H bonds—the P atoms are not connected to each other. The rest of the structure, however, is essentially the same as **VIII**—4R chains, charge-balancing NH₄⁺ cations, four-connected [Sn²⁺], P=O bonds on each P, etc. In the other structure, P atoms are linked, but water molecules, rather than charge-compensating cations, surround the chains. As a result, both P atoms need P–OH groups. The figure in ref 17a shows that one P atom has a terminal P=O as well (the distance between this O and a Sn must have been considered too long to be depicted) and the Sn is three-connected.²⁶ In **VIII**, Sn1–O3 = 2.474 Å; in $(\text{NH}_4)_2\text{Sn}(\text{HPO}_3)_2$, Sn–O(6) = 2.696 Å for the equivalent groups (Figure 18a).

Discussion

The 3R chain has received little attention with regard to extended frameworks, probably since it previously has been observed in only a few structures (examples include a layered tin(II) oxalate phosphonate,^{17c} a layered tin(II) phosphate,²⁷ a “strip”²⁸ and a layered Co(II) phosphate,²⁹ and a tubular³⁰ and a 3D Zn(II)

(26) Reference 17a lacks atomic coordinates and the Cambridge Crystallographic Data Centre does not have the information. Thus, some bond distances cannot be established.

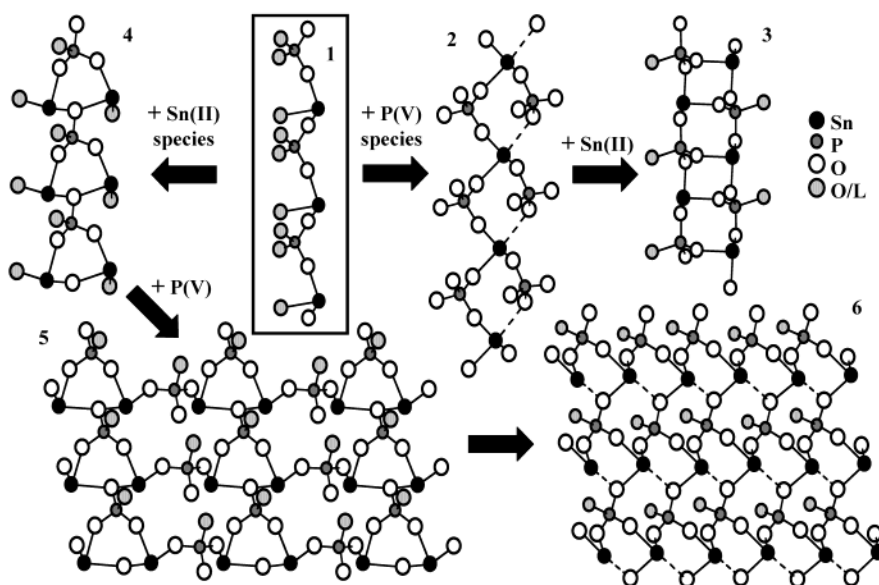


Figure 19. Evolution of tin(II) structures from an open-chain wire. Atoms in light gray (O/L^*) represent O^{2-}/OH^- groups in hypothetical intermediates or other ligands in known structures (see text). Dashed lines depict ($>2.5\text{ \AA}$) Sn- -O interactions.

phosphate³¹). SnPhPO_3 ,^{17d} SnHPO_3 ,^{18b} and $\text{SnPO}_3\text{F}^{22}$ have the same type of 6R layers (based on distorted 3R chains) found in **IV** and **V** and share similar unit cell parameters. The structure of the layered antimony(III) phosphonate $\text{Sb}_2\text{O}(\text{CH}_3\text{PO}_3)_2$ ^{32a} is like that of **IV** and **V**, and the three-dimensional structure of $\text{Sb}_2\text{O}(\text{O}_3\text{PCH}_2\text{PO}_3)_2$ ^{32b} is made of the same layers found in $\text{Sb}_2\text{O}(\text{CH}_3\text{PO}_3)_2$, just as **VI** is made of the same layers found in **IV** and **V**. (The differences between the Sn(II) and Sb(III) structures essentially arise from an oxygen bridge between two antimony(III) cations in the latter family of materials).

We suggest that a 3R chain may be a parent chain for the above SnPO, SbPO, ZnPO, and CoPO materials such as the progenitor 4R chain Ozin proposes for the AlPO family.¹¹ It is, however, difficult to visualize the formation of the 3-ring chain itself from condensation of individual molecular units⁹ or by transformation of corner-shared four-ring chains.^{11,28} Since both 3R and 4R chains are found in tin(II) and other metal phosphates, a common pathway for the formation of materials possessing either of these structural motifs might be possible. One such pathway is through condensation of metal centers with an open-chain (i.e., no rings) metal phosphate (MP) wire ($M/P = 1$). The idea of a wire exists as one of many possible hypothetical intermediates in the formation of AlPOs,³³ but the notion of it being a key intermediate has not been emphasized. Outlined

below is a possible mechanism for the formation of some metal phosphates through a MP wire.

Tin(II) Phosphates. The structure of **I** (Figure 2) would be analogous to the proposed wire intermediate, where the terminal chlorine, phenyl, and hydride groups that render **I** isolable would be replaced with reactive oxygen/hydroxyl groups (Figure 19, **1**). The recently reported $\text{M}[\text{SnF}(\text{HPO}_4)]$ ($\text{M} = \text{Na, NH}_4$)²⁰ has the same structure, with terminal hydroxo and oxo groups on the phosphorus and a terminal fluoride ligand on the tin(II). When a phosphorus species is added to **1** (Figure 19, **1** \rightarrow **2**), it could result in a "hanging wire" (Figure 19, **2**). $(\text{NH}_4)_2\text{Sn}(\text{HPO}_3)_2$ is analogous to such an intermediate between MP wires and MP_2 corner-sharing chains, with pendant phosphorus groups, reported to be hygroscopic and unstable in air.^{18a} The structure of $\text{Sn}(\text{HO}_3\text{PCH}_2\text{PO}_3\text{H})\cdot\text{H}_2\text{O}$ is nearly the same, where instead of terminal P-H, the phosphorus groups are connected through methylene units.^{17a} When we added a base and heated a mixture similar to that used by Zapf *et al.*,^{17a} we found $[\text{NH}_4]_2\text{Sn}(\text{O}_3\text{PCH}_2\text{PO}_3)$, **VIII** (Figure 18), where charge compensation is provided by ammonium cations rather than by protons of terminal hydroxyl groups. An O of the phosphorus species is closer to Sn in **VIII**, giving the material with the MP_2 corner-sharing structure (Figure 19, **2**, when dashed lines are considered). These corner-sharing chains might then go on to make larger structures or rearrange according to the scheme for AlPOs provided by Ozin and co-workers, to give edge-sharing M_2P_2 ladders (Figure 19, **2** \rightarrow **3**).¹¹ An M_2P_2 ladder analogue, $\text{Sn}(\text{PO}_3\text{CH}_2\text{COOH})$, **VII** (Figure 16), was isolated, where the organic group of the phosphorus species and the lone pair of electrons on tin(II) restrict growth at the positions where oxygens/hydroxyls would be found in intermediates (Figure 19, **3**). In addition, a layered polymorph of $\beta\text{-SnEtPO}_3$ (**IV**) is based on Sn_2P_2 4Rs.^{17b}

(27) Berndt, A. F.; Sylvester, J. M.; Jordan, T. H.; Spenger, T. F. *J. Appl. Crystallogr.* **1972**, *5*, 248.

(28) Rao, C. N. R.; Natarajan, S.; Neeraj, S. *J. Am. Chem. Soc.* **2000**, *122*, 2810.

(29) Choudhury, A.; Natarajan, S.; Rao, C. N. R. *J. Solid State Chem.* **2000**, *155*, 62.

(30) Choudhury, A.; Natarajan, S.; Rao, C. N. R. *J. Solid State Chem.* **2001**, *157*, 110.

(31) Neeraj, S.; Natarajan, S.; Rao, C. N. R. *Chem. Commun.* **1999**, 165.

(32) (a) Adair, B. A.; Guillou, N.; Alvarez, M.; Ferey, G.; Cheetham, A. K. *J. Solid State Chem.* **2001**, *162*, 347. (b) Adair, B. A.; Diaz de Delgado, G. D.; Delgado, J. M.; Cheetham, A. K. *Solid State Sci.* **2000**, *2*, 119.

(33) Oliver, S.; Kuperman, A.; Lough, A.; Ozin, G. A.; Garcés, J. M.; Olken, M. M.; Rudolf, P. *Stud. Surf. Sci. Catal.* **1994**, *84*, 219.

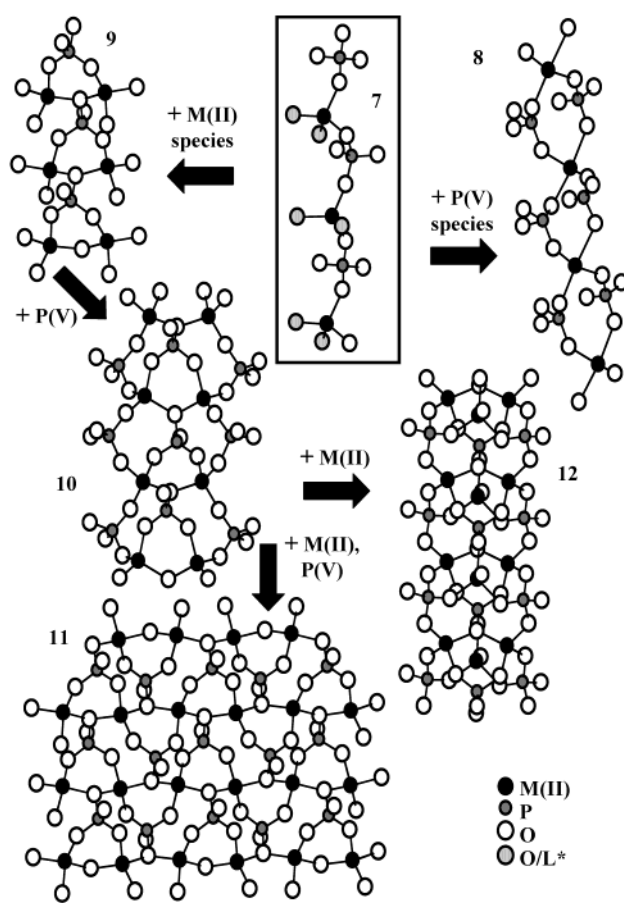


Figure 20. Evolution of M(II) structures from an open-chain wire. Atoms in light gray (O/L^*) represent O^{2-}/OH^- groups in hypothetical intermediates or other ligands in known structures (see text).

Instead of adding phosphorus species, a 3R M_2P chain like **II** could be formed when tin(II) solution species attack the MP wire (Figure 19, **1** \rightarrow **4**). Again, **II**, isolable under hydrothermal conditions, would be a stable analogue of this hypothetical 3R chain intermediate for the SnPO system, where the methyl group on the phosphorus and the chlorine group on the tin replace reactive oxygens/hydroxyls in the proposed intermediate. Structures **II**–**VI** suggest a building-up process involving the 3R chain (Figure 19, **4** \rightarrow **5**, **5** \rightarrow **6**), ultimately giving the three-dimensional network of **VI**.

Other Metal Phosphates. The isolation of (i) a zinc(II) phosphate wire, wherein methylimidazole is coordinated to the Zn^{2+} center;³⁴ (ii) a manganese(II) phosphate wire, with pendant HPO_4 and H_2PO_4 groups;³⁵ and (iii) an antimony(III) fluoride phosphate wire made from $[SbF_3O_2]$ and $[H_2PO_4]$ polyhedra,²¹ gives support to the proposal of the MP wire as an important intermediate in the formation of other metal phosphates

(Figure 20, **7**). Addition of phosphorus species to this wire could give the 4R MP_2 corner-sharing chains that are key to Ozin's reaction pathways (Figure 20, **7** \rightarrow **8**). These can then go on to make 4R ladders and larger extended structures. Alternatively, adding metal species to the wire would again give a 3R M_2P chain (Figure 20, **7** \rightarrow **9**) intermediate. This hypothetical 3R chain intermediate should have two reactive terminal oxygen/hydroxyl groups on the metal center (Figure 20, **9**) instead of one as in the tin(II) case (Figure 19, **4**). Though a structure analogous to **9** for four-connected metals has not been reported to the best of our knowledge, this 3R M_2P chain might still be significant in the case of metal-rich phosphate frameworks ($M/P > 1$) (Ozin's model has been applied to the formation of aluminum phosphates with $Al/P \leq 1$, restricted by Lowenstein's rule). This is because the M_2P_3 strip motif, found in $[C_4N_2H_{12}]_{1.5}[Co_2(HPO_4)_2PO_4]$,²⁷ is known. It is difficult to account for the formation of this structure by the rearrangement of 4R chains or ladders or by the linking of individual 4Rs. Adding more phosphorus species to the M_2P chain (Figure 20, **9** \rightarrow **10**) appears very plausible. This strip motif can grow to give layered²⁸ (Figure 20, **10** \rightarrow **11**), tubular²⁹ (Figure 3, **10** \rightarrow **12**), and 3D structures,³⁰ examples of which are all known.

Conclusion

This study not only illustrates a way to obtain various low-dimensional intermediates and relationships between them but also points toward a building-up mechanism involved in the formation of these materials. Variations in structure were obtained simply by changing the relative amounts of water and metal and phosphorus species, without the use of amines or other charge-compensating agents. We are exploring various metal phosphate/phosphonate/phosphinate systems to draw a more universal understanding of the formation of phosphate-based frameworks. For example, one of the authors has shown the reaction of phenylphosphinic acid with Zn ions yields a zinc phenylphosphinate³⁵ with a Zn_2P_2 4R corner-sharing chain, demonstrating this approach can be applied to other metal systems. The results suggest the relative reactivities of metal and phosphorus species toward the wire are critical in the formation of a specific structure.

Supporting Information Available: X-ray crystallographic data for structures **I**–**VIII** (CIF). This material is available free of charge via the Internet at <http://pubs.acs.org>.

CM020650X

(34) Ayi, A. A.; Neeraj, S.; Choudhury, A.; Natarajan, S.; Rao, C. N. R. *J. Phys. Chem. Solids* **2001**, *62*, 1481.

(35) Neeraj, S.; Cheetham, A. K., submitted.